Bioinspiration & Biomimetics

A biarticular passive exosuit to support balance control can reduce metabolic cost of walking

Hamid Barazesh[1] and Maziar Ahmad Sharbafi[1,2]

1. School of ECE, College of Engineering, University of Tehran, Tehran, Iran
2. Laufabor Locomotion Lab, Centre for Cognitive Science, Technische Universität Darmstadt, Hesse, Darmstadt, Germany

E-mail: barazeshhamid@ut.ac.ir and sharbafi@sport.tu-darmstadt.de

Abstract

Nowadays, the focus on the development of assistive devices just for people with mobility disorders has shifted towards enhancing physical abilities of able-bodied humans. As a result, the interest in the design of cheap and soft wearable exoskeletons (called exosuits) is distinctly growing. In this paper, a passive lower limb exosuit with two biarticular variable stiffness elements is introduced. These elements are in parallel to the hamstring muscles of the leg and controlled based on a new version of the FMCH (force modulated compliant hip) control framework in which the force feedback is replaced by the length feedback (called LMCH). The main insight to employ leg length feedback is to develop a passive exosuit. Fortunately, similar to FMCH, the LMCH method also predicts human-like balance control behaviours, such as the VPP (virtual pivot point) phenomenon, observed in human walking. Our simulation results, using a neuromuscular model of human walking, demonstrate that this method could reduce the metabolic cost of human walking by 10%. Furthermore, to validate the design and simulation results, a preliminary version of this exosuit comprised of springs with constant stiffness was built. An experiment with eight healthy subjects was performed. We made a comparison between the walking experiments while the exosuit is worn but the springs were slack and those when the appropriate springs were contributing. It shows that passive biarticular elasticity can result in a metabolic reduction of $14.7 \pm 4.27\%$. More importantly, compared to unassisted walking (when exosuit is not worn), such a passive device can reduce walking metabolic cost by $4.68 \pm 4.24\%$.

1. Introduction

Among different human gaits, walking is the most frequent activity in our daily life as humans walk about 10000 steps per day on average [1]. Therefore, developing assistive devices to support human walking is becoming a more popular research topic in robotics, biomechanics and rehabilitation research. Robotic devices for gait assistance can be divided into orthoses [2], prostheses [3] and exoskeletons [4]. Lower limb exoskeletons are mainly used for three types of applications [5]: (i) rehabilitation for patients with mobility disabilities [6–8], (ii) supporting patients with lost mobility in the lower extremity [9, 10], and (iii) improving the abilities of able-bodied humans by reducing energy consumption and increasing robustness against perturbations during walking

[11, 12]. In this paper, we address the last group concentrating on reducing the metabolic cost of transport.

Assistive devices for metabolic reduction are designed to work in active (powered) or passive manner. Studies on exoskeletons are mostly concentrated on active devices as they can increase the robustness of locomotion, which is crucial for impaired or elderly subjects, and the energy injection from actuators can generate high metabolic cost reduction in unimpaired people locomotion [13]. For example, Quinlivan *et al*, demonstrated the monotonic relation between assistance level (peak ankle moment) and net metabolic rate reduction in their exosuit [14]. In 2016, Mooney and Herr developed a powered ankle exoskeleton that could decrease walking metabolic cost by $11 \pm 4\%$ [15]. In the same year, Seo *et al* constructed a hip exoskeleton for seniors which could reduce energy consumption of walking by 13% [16]. A significant improvement

in metabolic cost reduction was achieved by human-in-the-loop-optimization method [13, 17]. With this method using metabolic rate feedback and Bayesian optimization, the energy consumption of walking was reduced by 24.2 ± 7.4% [13]. Recently, Kim *et al* developed an exosuit that could reduce the metabolic cost of both running and walking [18].

In the passive devices, metabolic reduction could be achieved by shifting the energy among different joints [19, 20] or storing and recoiling energy of the same joint over the gait cycle [21]. In this regard, without energy injection in passive devices, improving walking efficiency -which is already an efficient activity because of the evolution over thousands of years- is more challenging than in active devices. However, passive devices provide advantages such as requiring less maintenance and being light and economic, as they have no actuators, batteries, electronic boards, or sensors [21]. In 2015, Collins *et al* developed a passive elastic ankle exoskeleton working in parallel to the calf muscles that could reduce the metabolic cost of walking by 7.2 ± 2.6%, by assisting push-off [21]. More recently, Nasiri *et al*, demonstrated that energy transfer between two legs in their unpowered exoskeleton could reduce about 8% of energy consumption in running [19].

During the past few years, metabolic cost reduction by searching for optimal joint torques and controlling positive and negative work in specific joints has attracted researchers' attention [13, 21–23]. However, this is not the only way to support human gaits. Understanding biomechanics of human locomotion can help for designing assistive devices. In our previous studies, we found the potentials of using postural control and biarticular muscles for supporting human walking which can also result in metabolic cost reduction [24, 25]. In [26], we proposed a new approach to design and control a lower limb assistive devices. Based on the VPP (virtual pivot point) [27] concept as a bioinspired posture control method, the ground reaction force (GRF) was used to modulate the stiffness of a biarticular spring, parallel to the human hamstring (HAM) muscle [26]. Gait assistance with this FMCH (force modulated compliant hip) method could decrease metabolic cost of walking by 12% in a neuromuscular model of human walking [28]. Using leg force feedback to tune the biarticular spring's stiffness could be implemented in an either active or quasi passive exoskeleton (see an example of quasi passive exosuit in [29]). In this paper, the goal is to introduce such a bioinspired design for a passive exosuit. In that respect, we extend the previous method in different aspects: (1) *control:* introducing the LMCH (Length Modulated Compliant Hip) control concept in which the leg force feedback (GRF) for adjusting the biarticular (artificial) muscle stiffness is replaced by the leg length feedback, (2) *neuromuscular simulations:* introducing and testing a passive version of the FMCH-based exosuit, (3) *experiments:* (a) testing the effects of passive

biarticular springs without any feedback (b) adding a second biarticular spring mimicking the rectus femoris (RF) muscle in human legs. (4) *implementation:* introducing a mechanism to implement length feedback passively. The LMCH method is inspired by approximating human leg behaviour with a spring in different gaits [30, 31]. The simulation results demonstrated existence of VPP and 10 % reduction in metabolic cost of walking. In addition, our experiments demonstrate that significant reductions in metabolic cost are achievable by adding appropriate biarticular springs in the passive design.

2. Methods

The efficiency and performance of exoskeletons are dependent on the mechanical design principles, control architecture, and interaction between the robot and the human body. In that respect, human gait modeling can play an important role in predicting human reactions to the external forces (torques) and consequently in the design and control of assistive robots. Different detail levels can be considered in human gait modeling. One method for simplifying the understanding of human locomotion was suggested by the concept of locomotor subfunctions (i.e. stance, swing, and balance) [32]. We believe that such an abstract representation and the *template and anchor* [33] concept are useful approaches for understanding the underlying principles of biological legged locomotion, and then to design and control of assistive devices. Therefore, in this section, first, we present the template-based modeling used for design and control of our exosuit. We introduce the LMCH (length modulated compliant hip) method as a template model for balancing as one of the locomotor subfunctions. The balance subfunction is selected because it might need larger supports by the assistive device, compared to the two other subfunctions in healthy subjects. Then, we describe template-model-based gait assistance and how we apply the LMCH method to design our exosuit. Implementing the designed exosuit in the neuromuscular model of Geyer & Herr [28] is used to assess its performance in reducing metabolic cost in human walking. Finally, we describe our recently developed passive exosuit with biarticular thigh springs. The support level of this system is described by the experimental results. This device is the first step to develop an LMCH-based exosuit. A simple mechanism to physically implement the length feedback to tune biarticular muscle stiffness is represented in appendix.

2.1. Modeling approach
In this section, we briefly present the template-based modeling for bipedal walking with the focus on the balance locomotor subfunction. These approaches describe the basic concepts for designing our assistive devices (e.g. in [25, 26]). First, the SLIP (spring loaded

inverted pendulum) model and the linear relationship between leg force and virtual leg length as the key point in the LMCH-based exoskeleton design is discussed. Then, the VPP (virtual pivot point) and the FMCH (force modulated compliant hip) models are explained to predict postural control in human gaits which is the main concept for walking assistance in this paper. Extension of these template models for designing the exosuit is described in section 2.2.

2.1.1. Template models

Template models are abstract representations of intricate systems describing the basic characteristics of locomotion [33]. Because of their simplicity and adequacy to represent complex behaviors, templates are regarded as useful tools in the study of legged locomotion. The spring-loaded inverted pendulum (SLIP) is one of the most well-known template models used in studying legged locomotion [30, 34]. This model is developed based on the linear force-length relationship of the stance leg, observed in different gaits [31, 35]. In the SLIP model, the body is modeled by a point mass at the center of mass location and the leg is modeled as a massless linear spring as shown in figure 1(a). The spring is located between the center of mass (CoM) and the center of pressure (CoP) of the foot. This model is shown to be advantageous in explaining gait characteristics like GRF pattern and CoM displacement in hopping [30], running [36] and walking [31]. The SLIP model is the basic element of our modeling. However, the spring-mass mechanism in the SLIP model can mainly explain the stance locomotor subfunction in human gaits, but for other subfunctions, such as swing or balance, it needs further extensions [37, 38].

2.1.2. VPP model for human posture control

The evolution from quadrupedal to bipedal locomotion, though considered as a great evolution in humans, creates the problem of posture control. The first step to address this is to study bipedal template models that can inherently represent upper body balance. For that, the SLIP model was extended to include a rigid trunk. This model is known as TSLIP [39]. This way, upright posture, which has a key role in stabilizing human locomotion can be predicted by template models. The method that explains upright posture in humans is the virtual pivot point (VPP) proposed in [27]. According to this concept, humans intend to keep their upper body vertical during walking. Analyzing human walking in the sagittal plane shows that the ground reaction forces (GRF) are intersecting at a point (called VPP) above the center of mass. Redirecting the GRFs through this virtual pivot point can replicate the oscillatory movement of a virtual pendulum with concentrated mass at CoM hanging from VPP [27]. This virtual pendulum can predict human posture control in walking. It is shown that in the TSLIP model, the required torque at the hip

joint for establishing VPP and achieving stable walking is calculated as follows

$$\tau_{\text{VPP}} = F_s \, l \, \frac{d_h \sin\psi + d_{\text{VPP}} \sin(\psi - \gamma)}{l + d_h \cos\psi + d_{\text{VPP}} \cos(\psi - \gamma)}, \quad (1)$$

where F_s, l, d_{VPP} and d_h are leg force, leg length, distance between VPP and CoM, and distance between CoM and hip joint, respectively. In addition, ψ and γ, respectively, denote the angle between the trunk and the virtual leg (the line between hip and CoP) and the angle between the body axis and the vector from CoM to VPP, as shown in figure 1(b).

2.1.3. FMCH model

This *force modulated compliant hip* biomechanical model was introduced to physically implement the VPP concept in running [40] and walking [41]. In this bioinspired model, a variable spring between the leg and upper body is considered to generate hip torque (see figure 1(b)). The stiffness of this spring is adjusted by the leg force feedback

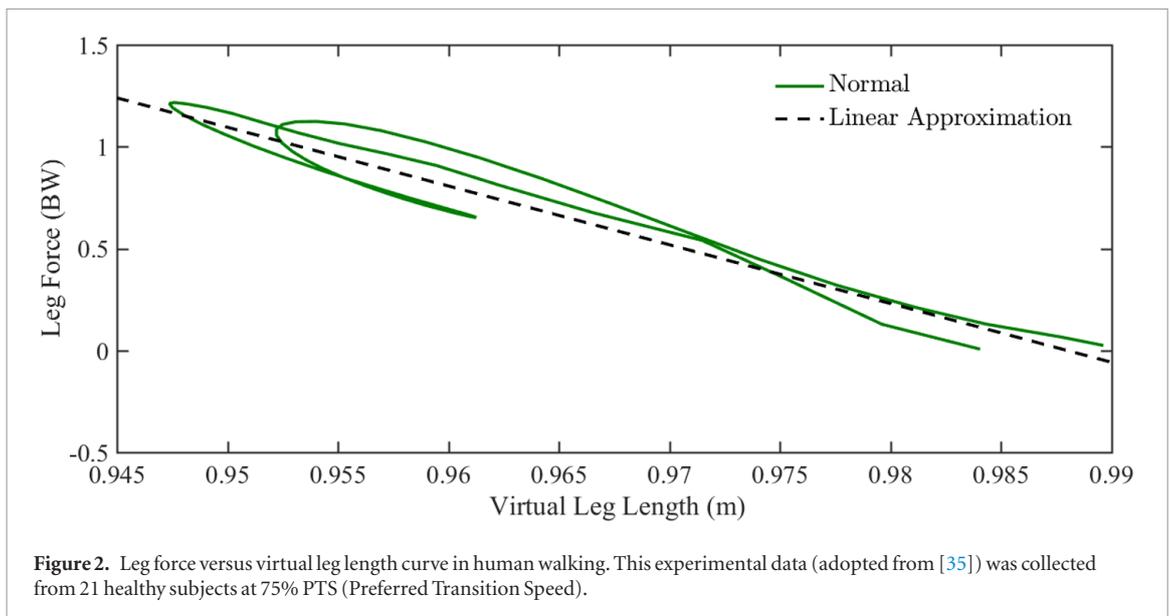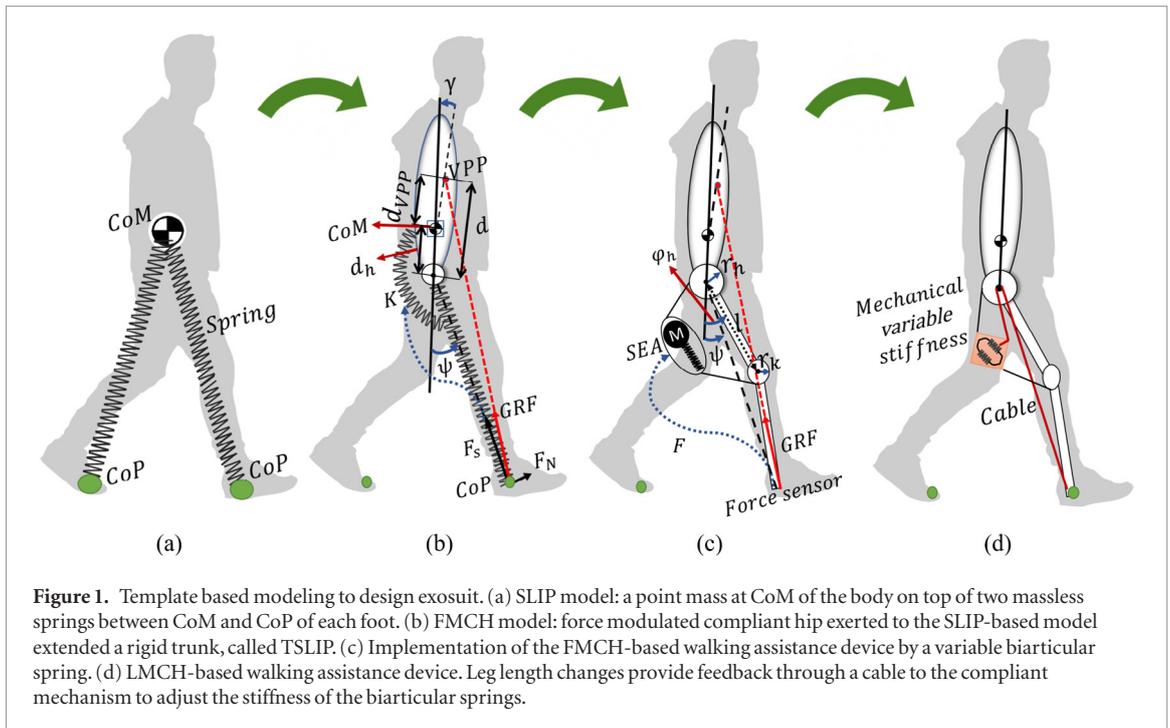$$\tau = k \frac{F_s}{W}(\psi - \psi_0) = k F_s^N (\psi - \psi_0), \quad (2)$$

in which W, F_s^N, k and ψ_0 are the bodyweight, normalized leg force, hip spring stiffness and rest angle, respectively. Dividing F_s by W to define the normalized leg force (as used in figure 2) makes the units consistent. It was shown that this model provides a precise approximation of VPP torque (with less than 2% error) [41]. In the FMCH model as well as the VPP model, we do not need to measure the trunk angle with respect to the ground for keeping the body in a vertical position. Furthermore, since a variable stiffness mechanism provides the torque proportional to the angle intrinsically, we do not need to measure the angle between the upper body and the virtual leg in the FMCH method. By replacing the spring with the Hill-type muscle model [42], Davoodi *et al*, demonstrated that the FMCH model is compatible with the human muscular system and can predict human balancing through neuromuscular modeling [43].

2.2. Model-based gait assistance

In this section, we first extend the FMCH concept to be applicable for gait assistance. For this, we explain the extension of the FMCH model to a segmented mechanism. This extension provides the infrastructure of the exosuit to support biarticular thigh muscles in order to reduce metabolic cost in walking. Further, we discuss the implementation of replacing leg force with leg length feedback in a passive exosuit.

2.2.1. FMCH-based gait assistance

As previously mentioned, the FMCH presents a model of human walking comprised of two virtual hip springs and two virtual legs connected to a trunk. It is noteworthy to mention that this so-called virtual hip spring resembles the human biarticular muscles

Figure 1. Template based modeling to design exosuit. (a) SLIP model: a point mass at CoM of the body on top of two massless springs between CoM and CoP of each foot. (b) FMCH model: force modulated compliant hip exerted to the SLIP-based model extended a rigid trunk, called TSLIP. (c) Implementation of the FMCH-based walking assistance device by a variable biarticular spring. (d) LMCH-based walking assistance device. Leg length changes provide feedback through a cable to the compliant mechanism to adjust the stiffness of the biarticular springs.

Figure 2. Leg force versus virtual leg length curve in human walking. This experimental data (adopted from [35]) was collected from 21 healthy subjects at 75% PTS (Preferred Transition Speed).

(such as hamstring (HAM)), if the hip-to-knee lever arm ratio is adjusted properly [44]. In our previous exosuit design [26], a biarticular actuator—placed in parallel to the biarticular HAM muscle for upper body posture control—was considered to mimic the behavior of an adjustable spring. Hereafter, we name this adjustable parallel spring, the *augmented spring (AS)*. The stiffness of this spring (similar to the virtual hip springs in the FMCH) is adjusted by the leg force feedback. Thus, the generated force of the augmented spring can be written as:

$$F_{AS} = k_a F_s^N (l_{AS} - l_{AS0}) = k_a F_s^N \Delta l_{AS}, \quad (3)$$

in which, l_{AS} and l_{AS0} are the augmented spring's length and rest length, respectively. Here, k_a and l_{AS0} can determine the amplitude and width of the assistive force, respectively. Thus, these parameters are

considered as tuning parameters to find the optimal assistive force pattern.

In the biarticular configuration illustrated in figure 1(c), the spring length change Δl_{AS} can be calculated based on the deviation of the knee angle ($\delta\varphi_k$) and hip angle ($\delta\varphi_h$) from a rest position (when the spring does not produce force), as follows,

$$\Delta l_{AS} = r_h \Delta\phi_h - r_k \Delta\phi_k \quad (4)$$

where r_k and r_h are the lever arms of knee and hip joints, respectively (see figure 1(c)).

In [26], we showed that by setting the hip to knee lever arm ratio to 2, the augmented spring length changes (Δl_{AS}) will be proportional to the virtual hip angle changes ($\Delta\psi$)

$$\Delta l_{AS} = r_h \Delta\psi. \quad (5)$$

This means that the model with a segmented leg and biarticular springs adjusted by leg force mimics the FMCH hip joint control, given by equation (2). This relation is obtained from having thigh and shank segments of the same length. Therefore, by installing a biarticular actuator including knee and hip joints (with hip to knee lever arm ratio equal to (2)), the assistive device based on the FMCH concept can be implemented.

2.2.2. LMCH-based gait assistance

By investigating the dynamic behavior of human walking, one can find out that the relation between the leg force and virtual leg length can be considered as a linear function. Figure 2 shows the virtual leg force-length curve in human walking at normal speed 75%PTS[3] based on human experimental data [35]. This data was collected from treadmill walking of twenty-one healthy subjects (11 female, 10 male, age: 22–28 yrs, height: 1.64–1.82 m, weight: 59.2–82.6 kg) [35]. According to figure 2 the force-length curve can be approximated by a line (black dashed line). This figure shows that the assumption of considering a linear spring (e.g. in the SLIP model) between the hip and CoP is acceptable. Therefore, the generated leg force can be approximated by the changes of the virtual leg length (distance from hip to CoP). Thus, in order to translate the FMCH-based exosuit design to a passive version, we substitute the leg force feedback with the virtual leg length, as seen in figure 1(d) in the length modulated compliant hip (LMCH) based exosuit. Measuring displacement can be easily performed by attaching the ankle to hip by a cable as a mechanical sensor to change the effective stiffness of the biarticular spring. This removes the need for having electronic sensors which was inevitable for force feedback in the FMCH-based gait assistance.

Developing a variable stiffness biarticular spring with sufficiently large stiffness range, rapid stiffness change and energy-efficiency (consuming no energy to hold stiffness and ability to change stiffness, even under mechanical load) is still a challenge in variable impedance actuator designs [45]. A passive mechanism to adjust the augmented stiffness of a biarticular spring by length feedback is suggested in appendix. The proposed mechanism has three interaction ports (this term is borrowed from impedance control concept [46]), in which the stiffness between two ports is adjusted by the position of the third input port. Because of the similarity between the functionality of this mechanism and transistors in electrical circuits, we call it *TransComp* (for Transistor like Compliance). Please find more information in appendix. All in all, force generation in the LMCH-based (passive) exosuit can be summarized by the following equation:

$$F_{AS}^{LMCH} = \overbrace{k\left(1 - \frac{L}{L_0}\right)}^{K}(l_{AS} - l_{AS0}). \tag{6}$$

Here, L, L_0, k and K denote the virtual leg length, the leg spring rest length, the normalized and the adjusted stiffness of the augmented spring (AS), respectively. The concept of LMCH-based gait assistance can be implemented by connecting a cable from the foot, passing through the hip joint, to the third input port of the TransComp. The other two input ports are attached to the upper body and shank, as shown in figure 1(d)

2.3. Implementation of LMCH-based exosuit in the Neuromuscular model

One approach for evaluating gait assistance with exosuits is investigating its effects on human energy consumption (metabolic cost) and muscles activation. Therefore, by analyzing these two metrics, we assess LMCH-based gait assistance in the neuromuscular model of Geyer and Herr [28]. For this, we considered an adjustable compliance in parallel with HAM which applies a force calculated by equation (6), with a hip to knee lever arm ratio of 2. Then, the external force was optimized so that the metabolic cost of walking is minimized. In the following, we will first briefly introduce the neuromuscular model [28], extended by adding the exosuit. Then, the optimization for finding the parameters of the exosuit is explained.

2.3.1. Neuromuscular model

This model includes seven segments (1 upper body, 2 thighs, 2 shanks, and 2 feet) and seven muscles for each leg; i.e. Hamstrings, Gastrocnemius, Vastus, Soleus, Gluteus Maximus, Hip flexor and Tibialis Anterior. The Hill-type muscle model is employed [42] and the muscles are activated based on the reflex control method (local feedback of muscle length/velocity/force) [28, 47]. This model was shown to be capable of mimicking human walking kinematics, kinetics, dynamic and muscle activation in diverse situations [48].

Since this model works based on reflex control, it can be considered as a responsive model to predict human reactions to external forces such as the effects of adding an assistive device. In our simulations, we do not update the reflex gains in the neuromuscular model after adding the exosuit. With the fixed neuromuscular model, if the walking metabolic cost is reduced while the movement patterns do not significantly change, it is expected that optimization of the reflex gains will result in higher reductions in human energy consumption. Therefore, the outcomes of this study could be a sub-optimal solution which can even be improved if the wearer can properly adapt to the exosuit. For implementing the exosuit in the neuromuscular model we added an actuator between upper body and the shank. Similar to the HAM muscle this actuator can generate hip extension and knee flexion torques. We calculate the leg length (L) and actuator

---

[3] Preferred transition speed from walking to running.

length (l_{AS}) to produce the force given by equation (6). Then, this force was applied to the hip and knee by multiplying with 0.1 (m) and 0.05 (m) to provide a lever arm ratio of 2.

2.3.2. Optimization

In order to find the maximum assistance to human walking (in the neuromuscular simulation model) in terms of reducing metabolic cost, we optimized the LMCH control parameters. According to equation (6), the tuning control parameters that should be optimize are L_0, k, and l_{AS0}. The first constraint for optimization is walking stability with the desired speed. Here, we use the step-to-fall method to determine a stable gait. We define 50 steps without falling and a 5% margin for the average speed of 50 steps, as the stability criterion. For energy consumption minimization in the human body, the following cost function (J) is defined:

$$J = \frac{1}{M} \sum_{i=50-M+1}^{50} \frac{E_{met}^{total}}{d} \qquad (7)$$

where i denotes the ith step and E_{met}^{total} is the total metabolic cost during a walking step with CoM displacement d. Thus, J is the average consumed energy (per meter) in the last M steps. Here, E_{met}^{total} is calculated as follows:

$$E_{met}^{total} = \sum_{i=1}^{14} E_{met}^i. \qquad (8)$$

In this equation, E_{met}^i denotes the metabolic cost of each muscle. For ensuring that the system reaches a steady state, we calculate J for the last 30 steps ($M = 30$) and compare this cost function with and without assistance. The metabolic cost of each muscle E_{met}^i in equation (8) is computed by the following equation:

$$E_{met} = \int_{t_1}^{t_2} P_{met} \qquad (9)$$

where $P_{met}(t)$ is the metabolic rate [49] computed by:

$$P_{met}(t) = P(v_{CE}/v_{max}) \times A(t) \times |F_{max} \times v_{max}| \qquad (10)$$

in which $P(x)$ is a function of x that is approximated based on the empirical data [50]:

$$P(x) = \begin{cases} 0.01 - 0.11x + 0.06 \exp(23x) & x < 0 \\ 0.23 - 0.16 \exp(-8x) & x \geqslant 0 \end{cases}. \qquad (11)$$

For finding the optimal LMCH parameters, we use a global brute force search in a reasonable range that minimizes the value of J computed by equation (7). First, we found a reasonable parameter range for L_0 and k using a linear function of the leg length for approximating the GRF (leg force). For this, we used human experimental data from [35], as shown in figure 2. Employing the outcomes of implementing FMCH in our previous study [26] and these bounds, we found a reasonable range for all three parameters. A brute-force search with an appropriate resolution is sufficient to find the optimal value. Thus, the assistive

device with the optimized parameters minimizes the metabolic cost of transport.

2.4. Experiment

Our proposed concept is comprised of two main features: parallel thigh compliance and adjustable stiffness. In order to verify the effect of the first property in gait assistance, we developed a passive exosuit using biarticular springs with constant stiffness as shown in figure 3. For the second feature, we are developing the adjustable compliance with the TransComp mechanism which is under construction (see appendix for details). The exosuit consists of two silicone rubber bands resembling biarticular springs in parallel with HAM and RF muscles for each leg, called biarticular artificial muscles (BAM) hereafter. For implementing the compliant elements, we preferred rubber bands to metal springs, because they are soft and light weight which prevents discomfort resulting from the impact of the wobbling springs on the thigh. The higher ratio of (stored) energy/weight in the rubber bands compared to metal springs with he same stiffness is the underlying reason. In order to find appropriate stiffness range of the rubber bands (augmented spring), we performed experiments with two pilot subjects before the final experiments. We gradually increased the stiffness and asked them to walk on the treadmill. We found the minimum stiffness with which the subjects detected exosuit contribution and the maximum stiffness with which they did not feel uncomfortable. The range of stiffness (shown in table 1) for the final experiment is selected based on these values. The test subjects did not participate in the final experiment.

Figure 3 shows different elements and the structure of the exosuit. The whole mass of exosuit is 1.8 kg and it is comprised of four main parts: rubber bands, waist brace, shank brace and ankle brace. As can be seen in figure 3(a), we attached three braces to the body and the rubber bands (shown in red) are connected between the waist and shank braces with straps, to implement passive BAMs. Within this design the lever arms at the hip and the knee joints are about 0.2 m and 0.1 m, respectively. The ankle brace is fixed below the belly of the calf muscle and is connected to the shank brace with canvas straps. Its functionality is to avoid upward movement of the shank brace while being pulled up by BAMs. More information about different parts of the exosuit is presented in table 1.

Eight non-impaired male subjects (age, 23–26 years; mass, 60–87 kg; height, 170–185 cm) participated in the experiment. All subjects were healthy without any known neuromuscular injury or functional impairment. They had no previous experience of walking with the exosuit. They voluntarily signed an informed consent form approved by the Sport Science Research Institute of Iran.

In the experiments, metabolic rate was measured to assess how much energy expenditure can be reduced
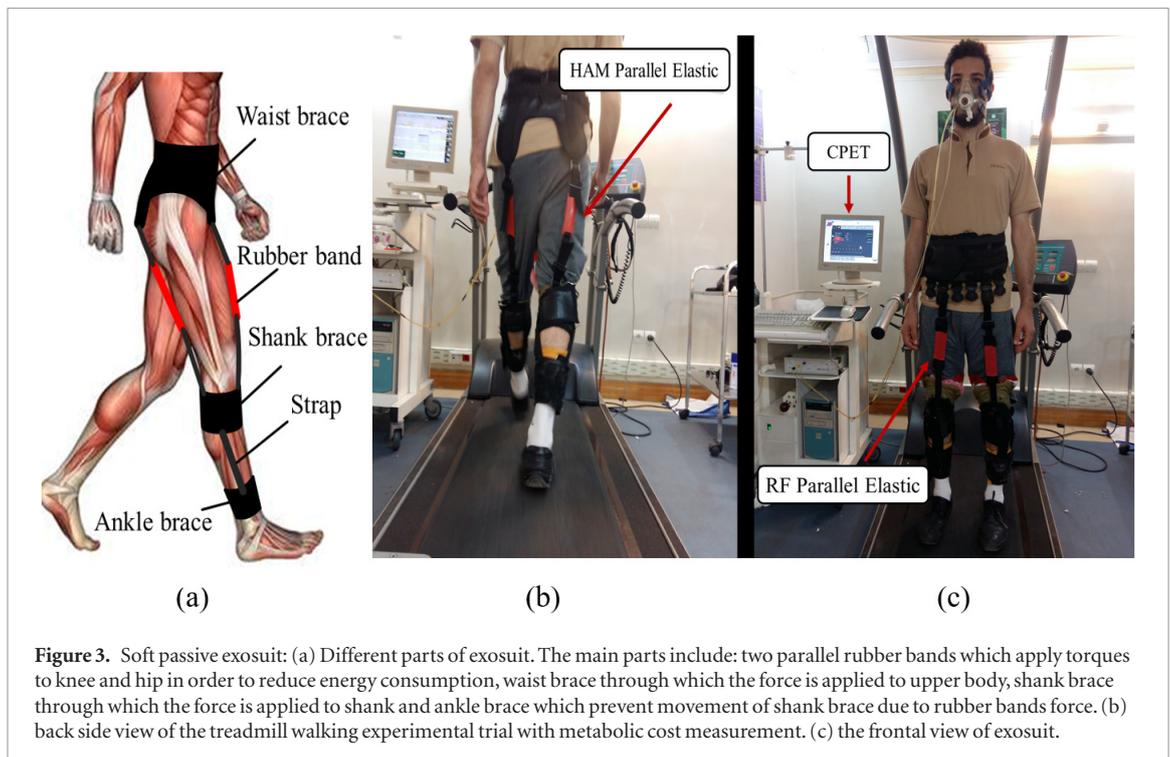
Figure 3. Soft passive exosuit: (a) Different parts of exosuit. The main parts include: two parallel rubber bands which apply torques to knee and hip in order to reduce energy consumption, waist brace through which the force is applied to upper body, shank brace through which the force is applied to shank and ankle brace which prevent movement of shank brace due to rubber bands force. (b) back side view of the treadmill walking experimental trial with metabolic cost measurement. (c) the frontal view of exosuit.
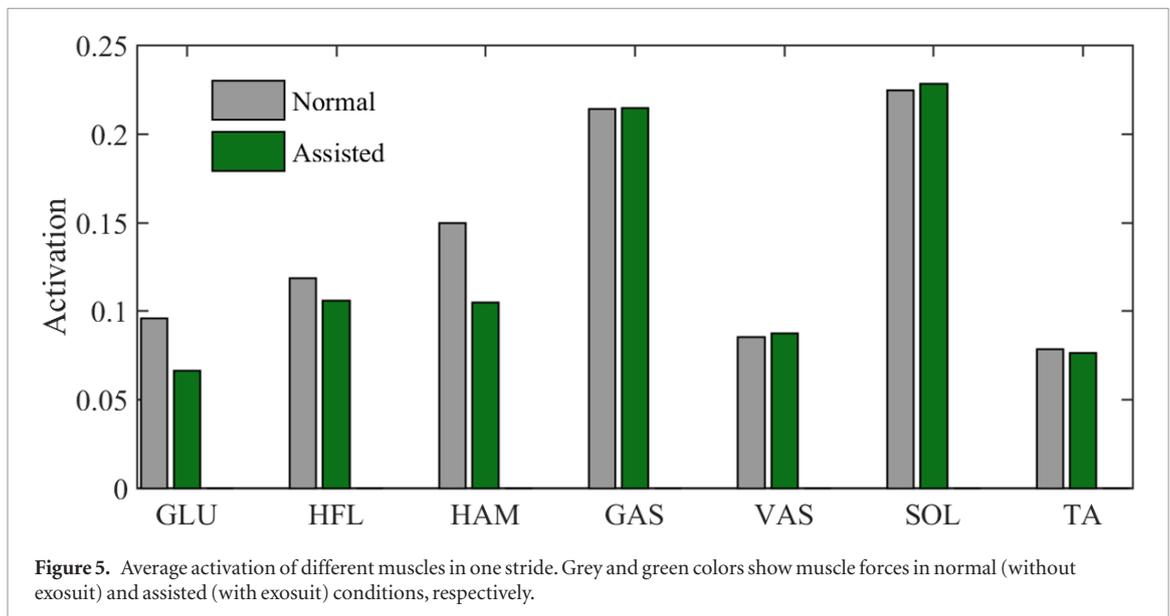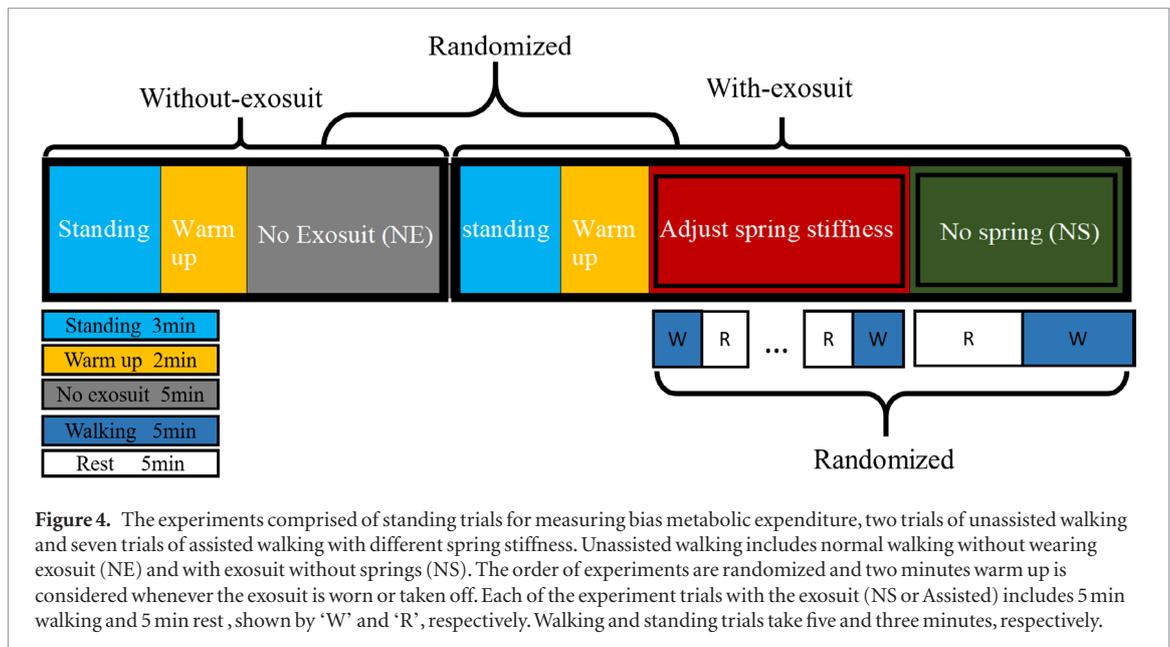
Table 1. Exosuit design specifications. The determined range for some of the parameters (instead of a fixed number) relates to different body size of the subjects.

Component		Mass (g)	Description
Brace	Waist	650	
	Shank	155	Textile and foam
	Ankle	100	
Augmented spring	Low stiffness, 700 N m^{-1}	50	Silicone rubber band with canvas straps
	Medium stiffness, 1500 N m^{-1}	53	rest length: $l_{AS0} = 46$–53 cm
	High stiffness, 2200 N m^{-1}	55	lever arms: $r_h = 18$–22 cm, $r_k = 9$–11 cm
Knee protector pad		160	Foam and Plastic
Straps		25	2 Canvas straps for each leg
Total mass		1780–1800	The difference is due the selected spring.

by the assistive controller. For this, at each experimental trial, Oxygen consumption rate ($\dot{V}_{O_2}$) and carbon dioxide output rate ($\dot{V}_{CO_2}$) were measured. All participants walked on a treadmill at 1.3 m s^{-1} under different conditions: *1) NE (No Exosuit):* normal walking without the exosuit, *2) NS (No Spring):* walking with the complete exosuit without connecting BAMs, and *3) Assisted:* with contribution of the springs. Here, we did experiments of walking with three different stiffness (low, medium, and high, described in table 1) for each of the biarticular artificial muscles. In order to find optimal stiffness, different combinations of these three stiffness were tested for each of the biarticular artificial muscles. For high stiffness in the HAM artificial muscle, we skipped medium and high stiffness in the RF artificial muscle (just considered low stiffness) because this combination limit limb movement for the subjects and made discomfort. Therefore, we tested

7 combinations for assistance (when the springs are involved). For each subject we selected the results of the assisted experiment with the lowest metabolic cost as the results of the *Assisted* case. These 7 conditions besides NE and NS cases made 9 different conditions for each subject.

The measured data is from five minute experiments for each walking condition. These nine conditions were randomized to avoid baseline, fatigue and learning effects. Switching between NE and the two other conditions (NS and *Assisted*) required wearing or taking off the exosuit preceded by two minutes warm-up walking. In addition, for measuring bias metabolic expenditure with and without the exosuit, we considered three minute standing to measure bias metabolic expenditure in the with- and without-exosuit experiments, separately. More details about the experiment protocol can be found in figure 4.

Figure 4. The experiments comprised of standing trials for measuring bias metabolic expenditure, two trials of unassisted walking and seven trials of assisted walking with different spring stiffness. Unassisted walking includes normal walking without wearing exosuit (NE) and with exosuit without springs (NS). The order of experiments are randomized and two minutes warm up is considered whenever the exosuit is worn or taken off. Each of the experiment trials with the exosuit (NS or Assisted) includes 5 min walking and 5 min rest , shown by 'W' and 'R', respectively. Walking and standing trials take five and three minutes, respectively.

Figure 5. Average activation of different muscles in one stride. Grey and green colors show muscle forces in normal (without exosuit) and assisted (with exosuit) conditions, respectively.

3. Results

3.1. Simulations

In this section, the simulation results of applying LMCH-based biarticular exosuit for assisting human walking at a moderate speed (1.3 m s^{-1}) are explained. We compare the muscle forces, muscle activation and metabolic costs of 'Normal' walking (no-exosuit) with the *Assisted* walking (with exosuit). Since gait kinematics and the walking speed do not change significantly which is enforced by optimization constraints, these results are not shown. The optimal values of tuning parameters are $L_0 = 2.2$ m, $k = 3850$ N m^{-1} and $l_{AS0} = 0.49$ m. Regarding the leg length (L) variations in the simulation model, adjusted stiffness will change between 2100 N m^{-1} and 2200 N m^{-1}. For comparing to the developed exosuit, this variable stiffness can be approximated by a fixed spring with $K = 2150$ N m^{-1}.

3.1.1. Muscle activation

The first effects of external forces should be observed in muscle activation. Figure 5 shows changes in muscles activities resulting from gait assistance. Since the proposed exosuit is designed based on the upper body balance concept, the muscles contributing to the hip joint such as HAM, GLU and HFL will have the most significant reduction. The changes in other muscles are negligible. The maximum reduction is observed in the HAM muscle. This is expected as the exosuit is designed to be parallel to the HAM muscle. To better analyze the reflected effects on this muscle, its activation is shown in figure 6 in a complete gait cycle. A considerable reduction is observed in the first 40%
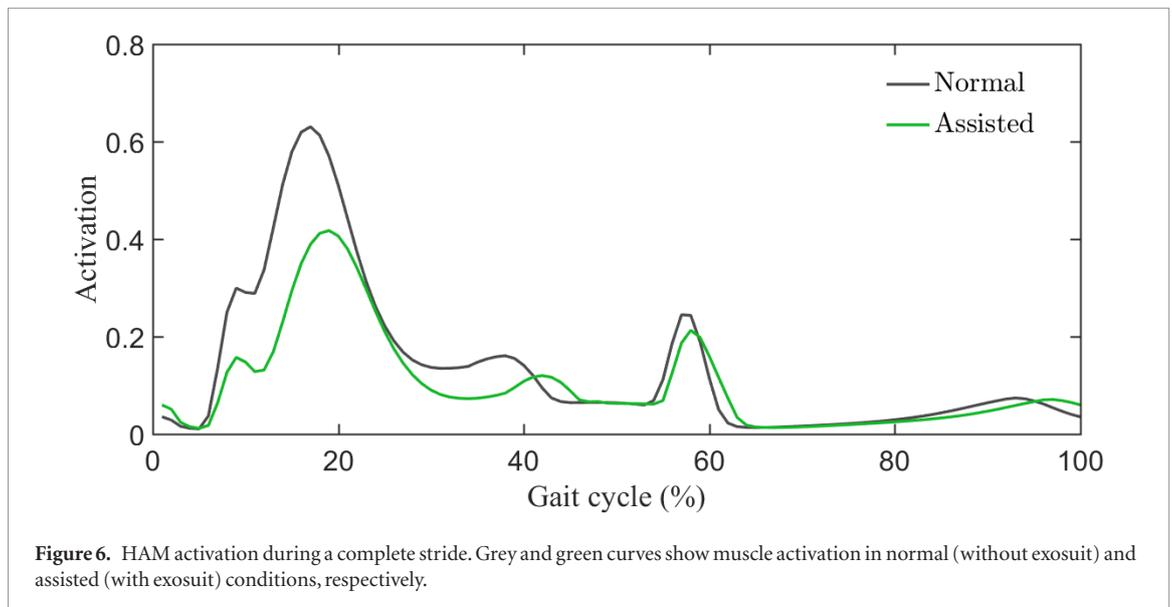
Figure 6. HAM activation during a complete stride. Grey and green curves show muscle activation in normal (without exosuit) and assisted (with exosuit) conditions, respectively.
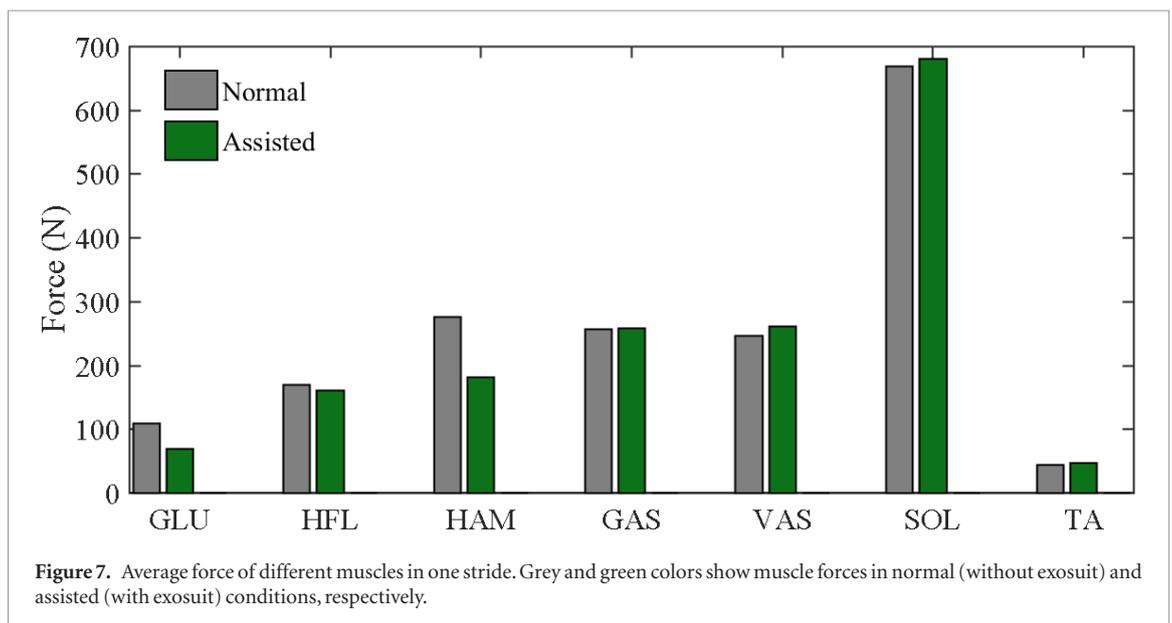

Figure 7. Average force of different muscles in one stride. Grey and green colors show muscle forces in normal (without exosuit) and assisted (with exosuit) conditions, respectively.
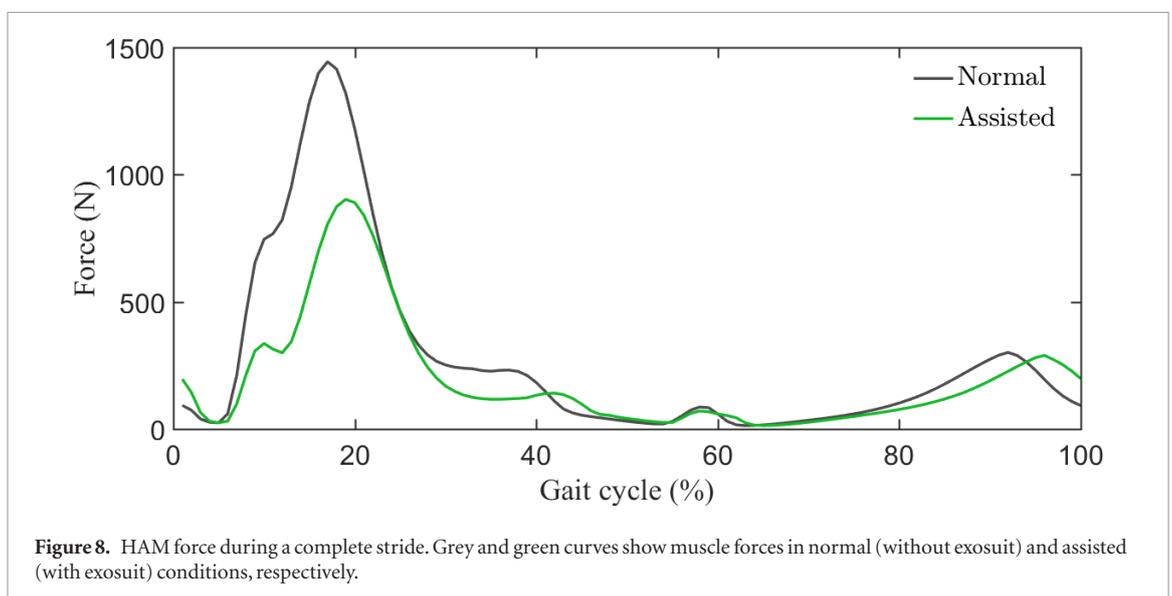

Figure 8. HAM force during a complete stride. Grey and green curves show muscle forces in normal (without exosuit) and assisted (with exosuit) conditions, respectively.

Figure 9. Average consumed energy (*J*) of different muscles for traveling one meter. Grey and green colors show *J* in normal (without exosuit) and assisted (with exosuit) conditions, respectively.

Figure 10. Total metabolic rate of a complete stride. Grey and green curves show metabolic rate in normal (without exosuit) and assisted (with exosuit) conditions, respectively.
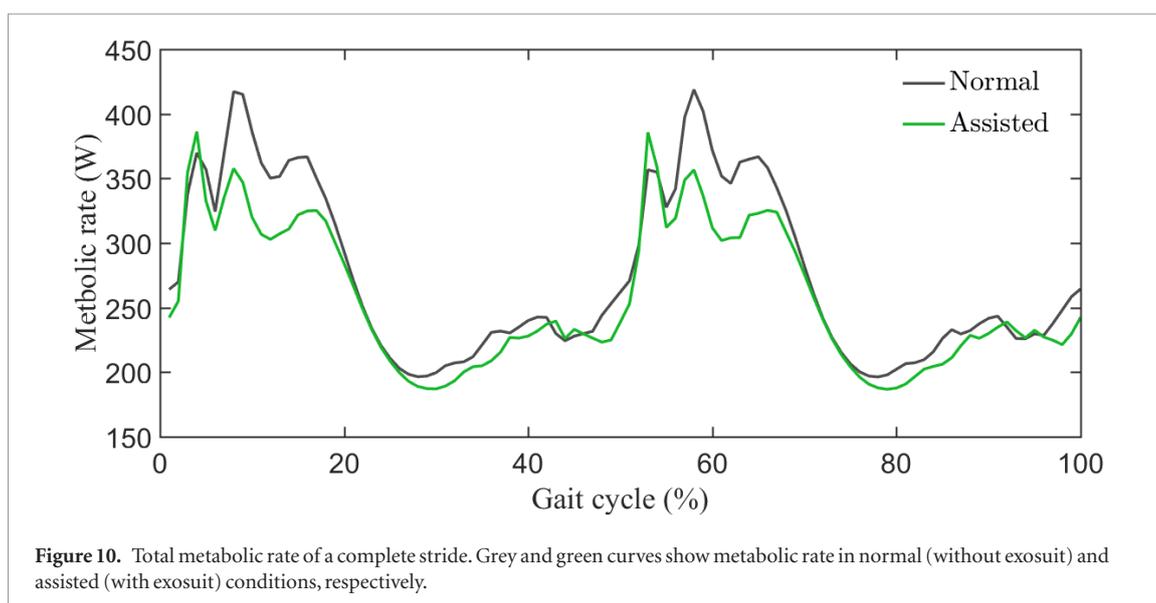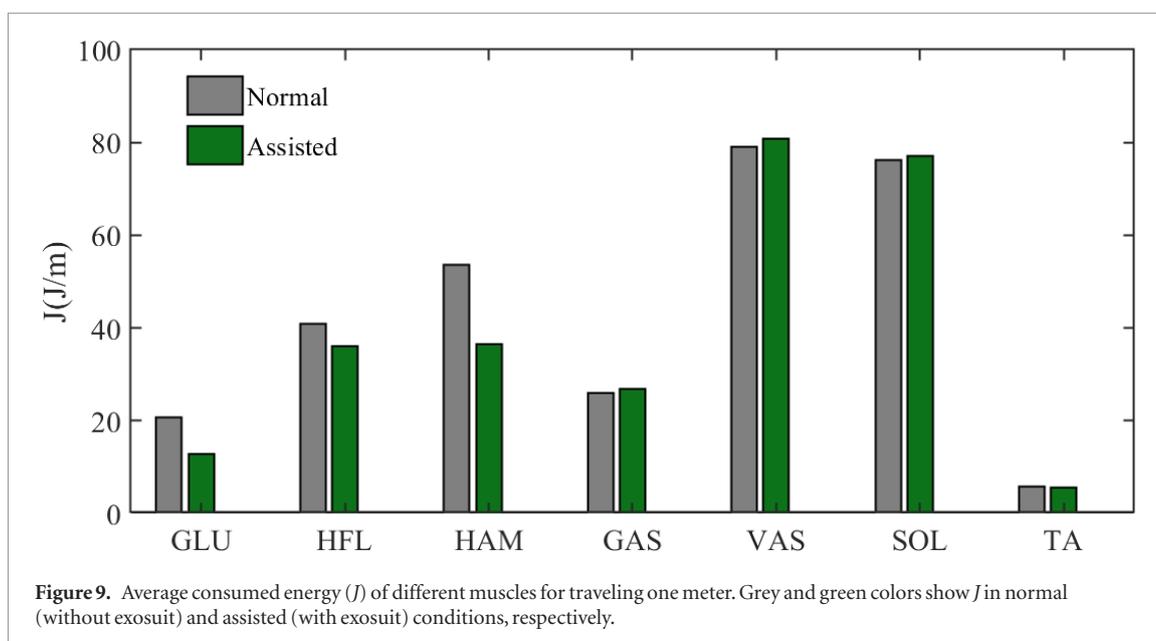
of the gait cycle in which the HAM muscle is the most active. These results support the design hypothesis of LMCH-based exosuit.
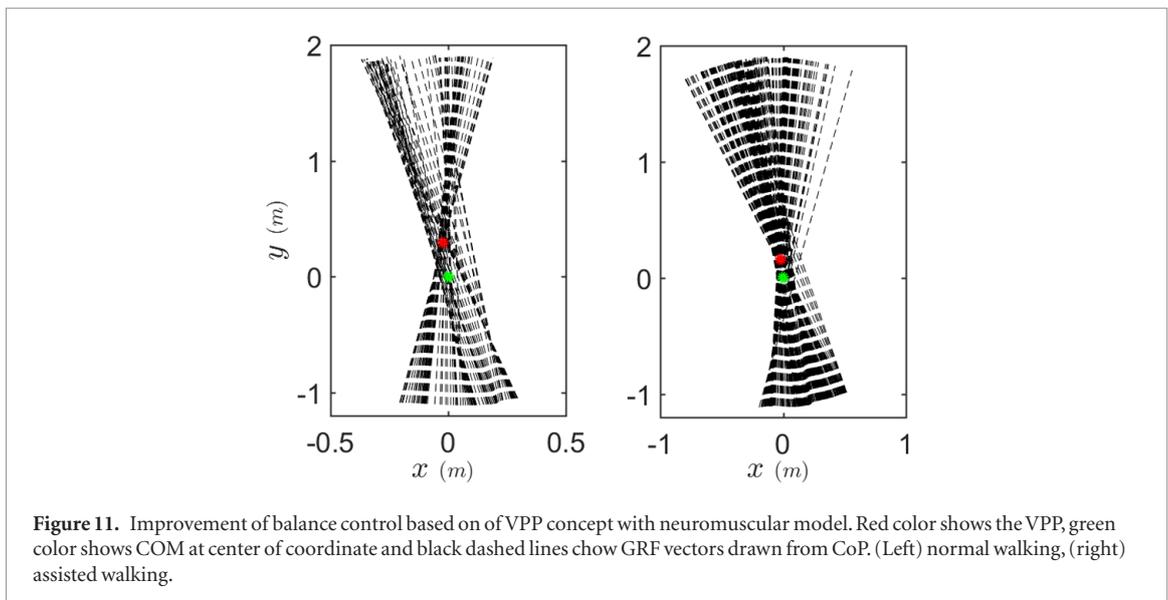
3.1.2. Muscle force

We know that muscle activation reduction is not equivalent to force reduction. However, based on the previously stated argument about the balance control design concept of the exosuit, we expect to have a similar reduction in muscles contributing to the hip joint. Figure 7 depicts significant reductions in HAM and GLU muscle forces, a small reduction in HFL muscle force, and a small increase in VAS and SOL muscle forces. In addition, the total generated force of all muscles is reduced which could result in lower energy consumption of the whole body. The HAM muscle force reduction during the gait cycle is shown in figure 8. With the large reduction in the peak force (about 40%), we expect less required peak power and less fatigue in this muscle.

3.1.3. Metabolic cost

Similar to muscle force and activity, we first show the consumed energy of each muscle per meter in figure 9. Once again, reductions in HAM, GLU, and HFL muscles are obtained with the assistive device, while there is an insignificant increase of about 3% in the VAS muscle. Changes in metabolic cost of other muscles are ignorable. From these results we expect reductions in total cost function (*J*) defined by equation (7). This value of metabolic cost for the full leg muscles is reduced by 10%.

Figure 10, shows the metabolic rate for normal and assisted condition during a gait cycle. In more than 70% of the gait cycle, the metabolic rate is decreased in assisted mode. In the first 20% of the gait cycle, a considerable reduction in metabolic rate is observed. This interval is when hamstring (that is parallel with exosuit) has its maximum activity and the hip extensor/knee flexor biarticular exosuit can significantly contribute to upper body balancing.

Figure 11. Improvement of balance control based on of VPP concept with neuromuscular model. Red color shows the VPP, green color shows COM at center of coordinate and black dashed lines chow GRF vectors drawn from CoP. (Left) normal walking, (right) assisted walking.

3.1.4. VPP as an index for posture control

The core concept of our LMCH-based exosuit design is inspired by the virtual pivot point (VPP) model. Thus, assistance by this exosuit should also improve balance control by providing a more focused VPP. Figure 11 depicts the GRF vectors in the coordinate system centered at CoM and aligned with upper body orientation while the VPP is shown with the red circle. The neuromuscular model for normal walking without assistance, predicts the VPP about 40 cm above CoM which is in line with finding in human walking at normal speeds. In the assisted case, the GRF vectors are more focused creating a clearer VPP. In addition, the distance between VPP and CoM is reduced.

3.2. Experimental results

In this section, we present the results of walking assistance with the passive exosuit, described in section 2.4. To investigate the effects of adding the biarticular springs, first, we compare the metabolic cost of the assisted test with no-Spring (NS). These results will be compared to normal (unassisted) walking which is called no-exosuit (NE). It is worth recalling that for each subject we selected the data of the assisted experiment (when the springs are contributing) with the lowest metabolic rate and the *Assisted* data is the average of these trials for different subjects. This way, we found the optimal stiffness arrangement for each subject (which might be different for different subjects) and selected it to assist that specific subject. Figure 12 presents the experimental results of the average metabolic rate for the last two minutes of walking subtracted by standing metabolic expenditure. Just by wearing the exosuit without contributions from the springs, the metabolic rate increases by $12.9 \pm 6.5\%$. This could be due to imperfect user-device interfaces and adding non-ideal wearable parts (e.g. braces) to the legs and the waist. Asbeck *et al* showed that additional mass in the legs could already increase metabolic cost by 8%/kg [51]. Interestingly, the comparison between
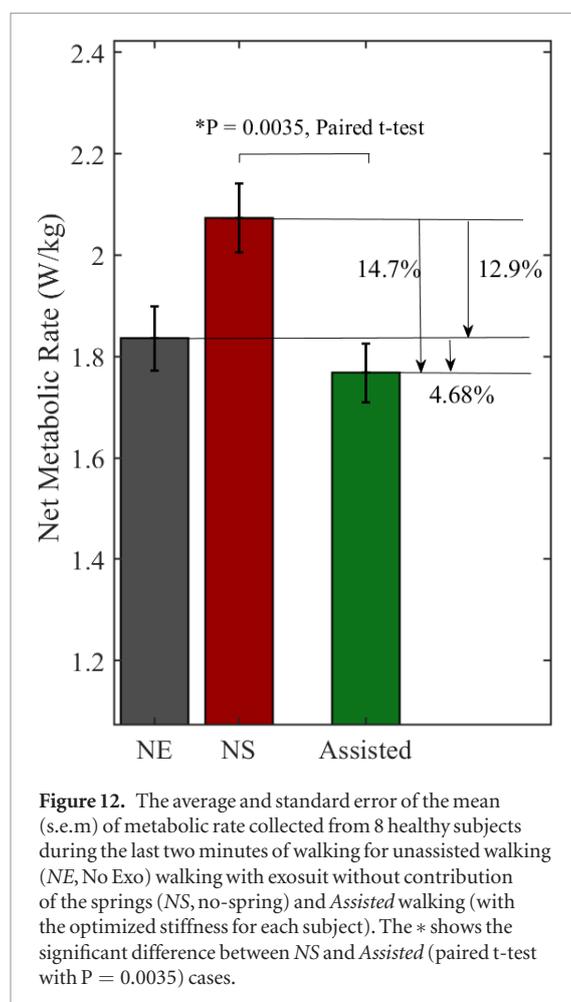
Assisted and NS shows that the optimal stiffness for the passive biarticular thigh artificial muscles results in a $14.7 \pm 4.27\%$ reduction in metabolic cost. These results support the statistically significant effect of the elastic element (the BAMs), approved by paired t-test with $P = 0.0035$. Therefore, the average metabolic rate of normal walking is reduced by $4.68 \pm 4.24\%$ using the proposed passive exosuit with the tuned stiffness.

4. Discussions

A new bio-inspired approach for designing assistive devices is presented in this paper. The proposed exosuit has lightweight, small size and low-cost design. Because of the muscle-like (flexible and tension-based) design of passive/active biarticular structures, their actuation in soft wearable assistive devices is growing [14, 52]. In that respect, we took advantage of the biarticular thigh muscle properties such as synchronizing adjacent joints without the need for sensory feedback [53], transferring energy between adjacent joints, passively [54] and providing access to GRF direction control with minor impact on the GRF magnitude [44]. This latter factor is very important for balance control [44].

4.1. Advantages of the LMCH-based gait assistance on modeling studies

To analyze the functionality and to identify optimal mechanical and control parameters of the exosuits, neuromuscular simulation models are employed [55]. In [26], Sharbafi *et al*, extended the neuromuscular walking model of [28] to evaluate the concept of gait assistance with an exosuit which has HAM-like actuators using the FMCH-based control. The results showed reductions of GLU and HAM muscle activity and 12% of the metabolic cost [26]. In this paper, we took one step further by replacing the force feedback with length feedback which can be used in passive assistive devices. The simulation results are comparable with those of the FMCH-based controlled

Figure 12. The average and standard error of the mean (s.e.m) of metabolic rate collected from 8 healthy subjects during the last two minutes of walking for unassisted walking (*NE*, No Exo) walking with exosuit without contribution of the springs (*NS*, no-spring) and *Assisted* walking (with the optimized stiffness for each subject). The ∗ shows the significant difference between *NS* and *Assisted* (paired t-test with P = 0.0035) cases.

exosuit of [26], regarding muscle activity, force, and metabolic costs. This outcome not only supports leg force approximation by a linear function of the virtual leg length [35], predicted by the SLIP model [30], but also confirms the applicability of such an approximation for simplifying the design and control of assistive devices. The results also show that reducing balance-related muscle activity does not considerably increase other muscles contribution, (below 3%), which will not yield side-effects such as muscle pain. The pronounced reduction in muscles which are contributing to the hip joint dominates such negligible increases. This validated our objective to assist balance control by paralleling a variable stiffness spring to the HAM muscle. By providing part of the required force during hip flexion and knee extension, we expect that this exosuit can compensate muscle weakness (observed commonly in injuries in sports such as soccer or basketball).

Since the LMCH (as an approximation of the FMCH) method is originated from the virtual pivot point (VPP), a bioinspired balance control concept, improved balancing was expected. Comparing VPP location before and after adding the exosuit showed a decrease in distance between VPP and CoM. This means the upper body has less oscillations with smoother posture control. Moreover, a more focused

VPP can be clearly found with assistance which supports the periodic movement of the upper body.

Investigating human gaits demonstrated that the length of the HAM muscle is not significantly affected by leg shortening or lengthening [56, 57], although it closely depends on the angle between the upper body and the leg. This means that the thigh biarticular muscles could play the role of sensors to measure the orientation of the limb axis directly. By this, using BAMs in the exosuit provides a simple solution of postural proprioception to support balance control. Within the LMCH approach, we couple the leg length to the upper body angle which means using *stance* locomotor subfunction to control *balance* locomotor subfunction. Synchronisation between different locomotor subfunctions is recently introduced under the *'concerted control'* concept [58]. In the concerted control, minimal sensory exchange is used to synchronize different locomotor subfunctions needless to have a central or supervisory control to manage coordination. Interpreting the LMCH in this context, could be presented as independent control of axial and perpendicular leg forces by mono- and biarticular muscles which is in line with studies on humans [59] and robots [44]. The modularity within the concerted control through assigning different locomotor subfunctions to different bi- and monoarticular muscles can be achieved by specific design parameters like the lever arm ratios in biarticular muscles. In humans, the hip to knee moment arm ratio in both thigh biarticular muscles are larger than one [60] (2 for HAM and 1.3 for RF muscle [61]). The ratio for our HAM-like BAM is also set to 2 in the design of our exosuit. This way, using biarticularity we benefit from modularity and with the leg length feedback we try to integrate the exosuit control into the human (concerted) motor control. The concerted control concept could be also investigated from other perspectives such as muscle synergies [62], in the future.

4.2. Advantages of biarticular compliance, based on experimental results

In order to evaluate the simulation results, a simplified version of the exosuit was built and tested in treadmill walking experiments. With the developed device we focused on the effects of constant BAMs (biarticular artificial muscles) while the mechanism for implementing length feedback was not completed to be usable in the exosuit. Instead, RF muscle was also assisted with the second BAM in the exosuit which was not investigated in the simulations (because the neuromuscular model of [28] does not include it). As described in the section 2, we selected the parameters range (rest length and stiffness) of the augmented springs of the developed exosuit based on human feedback, independent to the optimal values of the simulation study. Interestingly, the predictions of the simulation model ($K = 2150$ N m^{-1},

Figure 13. The BAExo (exosuit with biarticular thigh actuators) using SEA for both biarticular thigh actuators mimicking HAM and RF muscles in human body.

$l_{AS0} = 0.49$ m) comply with the experimental findings (($K = 700$–2200 N m^{-1}, $l_{AS0} = 0.46$–0.53 m). This shows that the findings of neuromuscular modeling could be used for estimating the operational range of the mechanical parameters.

The results support that with biarticular passive springs, the metabolic cost of walking can be reduced. It is worth noting that the considerable increase in metabolic cost of the normal walking (NE, no-exosuit) only by wearing the exosuit, when the springs were not contributing (NS, no-spring), demonstrate the inefficient design of the wearable parts e.g. with additional mass and uncomfortable attachment mechanism to the body. An improved design is required to reduce such issues in future. In spite of about a 13% increase in the metabolic cost, the involvement of artificial biarticular thigh muscles (elastic bands) could result in reduced energy consumption even compared to normal walking. In other words, these passive elements not only compensate the effect of imperfect design, but also provide additional benefits (close to 5% improvement) for walking efficiency. Nevertheless, we could not find a specific combinations of RF and HAM stiffness which could reduce the metabolic cost compared to unassisted walking (NE case). Therefore, further enhancements in the mechanical design of our exosuit is required to make the achievements more comparable with the state-of-the-art of passive exoskeletons e.g. [21] with 7% and [19] with 8% reduction.

Assistive devices usually aim at improving locomotion energy economy by supporting the joint torque or mechanical work. Recently, Beck *et al* [63] have shown that the energy consumption of walking is improved if the active muscle forces are reduced. Hence, the walking assistive devices should target supporting muscle force, rather than the joints' moment or mechanical work. In our passive exosuit, providing part of the forces which is supposed to be produced by human RF and HAM muscles, could result in decreasing active muscle volume which looks to be the main factor for improving locomotion economy [63]. This new point of view to predict human metabolic cost function based on muscle active volume [63] can also describe metabolic cost reduction in other passive devices [21, 19] which can be approved by measuring muscle functionality e.g. by ultrasonography.

By applying impulse-like pitch perturbations to the upper-body during standing, Schumacher *et al*, demonstrated that biarticular thigh muscles are the main contributors to balance control by having the largest increase in activation [64]. Further investigation of muscle functioning in locomotion shows RF length increases in the late stance which supports initiating leg swinging together with a concentric contraction [65]. In a reciprocal manner, the HAM muscle produces force by stretching in the second half of swing phase which generates leg retraction just before touchdown [66], followed by supporting hip extension in early stance phase [65]. With a similar working principle to the functionality of human biarticular thigh muscles [67], our passive exosuit can assist walking by exchanging energy between knee and hip joints and also between stance and swing phases.

4.3. Future outlook

In the here presented experiments, we only tested three stiffness values for each of the biarticular springs. Recently, Human-in-the-loop-Optimization (HILO) is introduced as a practical tool to optimize control parameters in the assistive devices [13]. This method can be used in the future to find the optimal stiffness

with the here presented exosuit. The next step of this study is extending the developed exosuit based on the LMCH concept. We expect that passive tuning of the biarticular thigh muscle compliance using the leg length could further increase metabolic reduction. Stiffness adaptation in human muscles has been already observed in walking [68, 69]. Furthermore, in our simulations the second BAM to support RF was not implemented (due to limitations in the model) whereas the experiments and our recent analysis in OpenSim confirm advantages of adding such an element. In [70], biarticular springs with constant stiffness was used to mimic swing leg motion in human walking. In a recently developed exosuit, we combined the FMCH-based adjustment of BAM stiffness in the stance phase with constant stiffness approach of [70] and tested that with an experiment-based model in OpenSim [24]. This method was also evaluated through implementation on the newly developed exosuit (called BAExo, shown in figure 13) and preliminary outcomes support the core control concept of using biarticular adjustable compliance. This setup can be also used to test LMCH-based control as a proof of concept.

Benefiting from biological studies in design and control of assistive devices are growing in recent years, e.g. with bioinspired morphological design [14, 22, 71], neuromuscular models [72] and applying HILO [73]. Our study also introduces a novel bioinspired approach for design of the passive assistive device. With the proposed abstraction of the complex neuro-mechanical interaction between different contributors to locomotion in the human body (e.g. motor neurons, muscles) a simplified solution for application in gait assistance is introduced. With this approach, we can benefit from inherited biological design and control concept in a practical way to develop a cheap device for a large number of users and not only impaired people.

The study presented here demonstrates the demand of future research to address technological challenges in the broad range of applications to benefit from (theoretical) potentials of biarticular actuation. Studies that apply biarticular mechanisms on assistive devices to support different locomotor subfunctions as well as synchronise between subfunctions should be addressed in the future and should evaluate features other than locomotion economy, such as walking stability.

Acknowledgment

Appendix. Suggested design of TransComp

There is a debate about ideal actuators, but an ideal variable stiffness spring actuator should have compact design, large stiffness range and rapid stiffness change, require no energy to keep stiffness, and be able to change stiffness under mechanical load [45]. Different designs are introduced for variable impedance actuators (VIA, e.g. Maccepa [74]), but still, no winning solution is known [75]. In addition, building a variable actuator which behaves as a biarticular muscle is a bigger challenge. The two issues are the tensile-based force generation and the influence across two joints. For example, in many of VIAs (such as Maccepa) the stiffness is tuned by changing the lever arm of the intercoupled spring (see more examples in [75]). This technique is not applicable for biarticular muscle-like actuators, as the level arm of both sides of the actuator should change simultaneously without changing the ratio between them. Moreover, for implementing the LMCH passively, we want to connect the leg length (e.g. by a cable) to the VIA for adjusting the stiffness, without using motors inside the actuator. For this, though different mechanisms can be employed [76], here we introduce the TransComp as a conceptual design to implement length based compliance modulation.

The proposed mechanism has three interaction (input) ports which will be pulled by cables as shown in figure A1. The TransComp is comprised of a frame which is connected by 4 cables to the inner mechanism. The inner mechanism has two springs which are connected in parallel by two bars. The bars could move inside two sliders which are connected to Port 1 and Port 2. These two ports should be attached to the upper body and the shank to support the biarticular thigh muscles. A cable which is going through Port 3 will behave as the leg length measurement system. By pulling this cable (to the right in figure A1) the measurable stiffness between Port 1 and Port 2 becomes closer to K_2. Because of connecting the inner mechanism to the frame by spring K_3, releasing the cable of Port 3 (which happens when the knee is bent) results in the movement of the inner mechanism in the opposite direction (leftward in figure A1). This way the resulting stiffness between Port1 and Port 2 becomes closer to K_1. By setting $K_1 \gg K_2$, leg shortening and lengthening will result in stiffening and softening the biarticular compliance, as suggested in the LMCH-based gait assistance. A simple experiment with the developed device is shown in figure A1(right). We hanged a 1 kg weight (10 N) from Port 2 when Port 1 was connected to a fixed point on the table. By pulling and releasing the cable connected to Port 3, the stiffness between Port 1 and Port 2 is changed which results in the displacement of the weight. Since the force direction in Port 3 is (almost) perpendicular to the delivered force by the variable stiffness (felt between Port 1 and Port 2), the
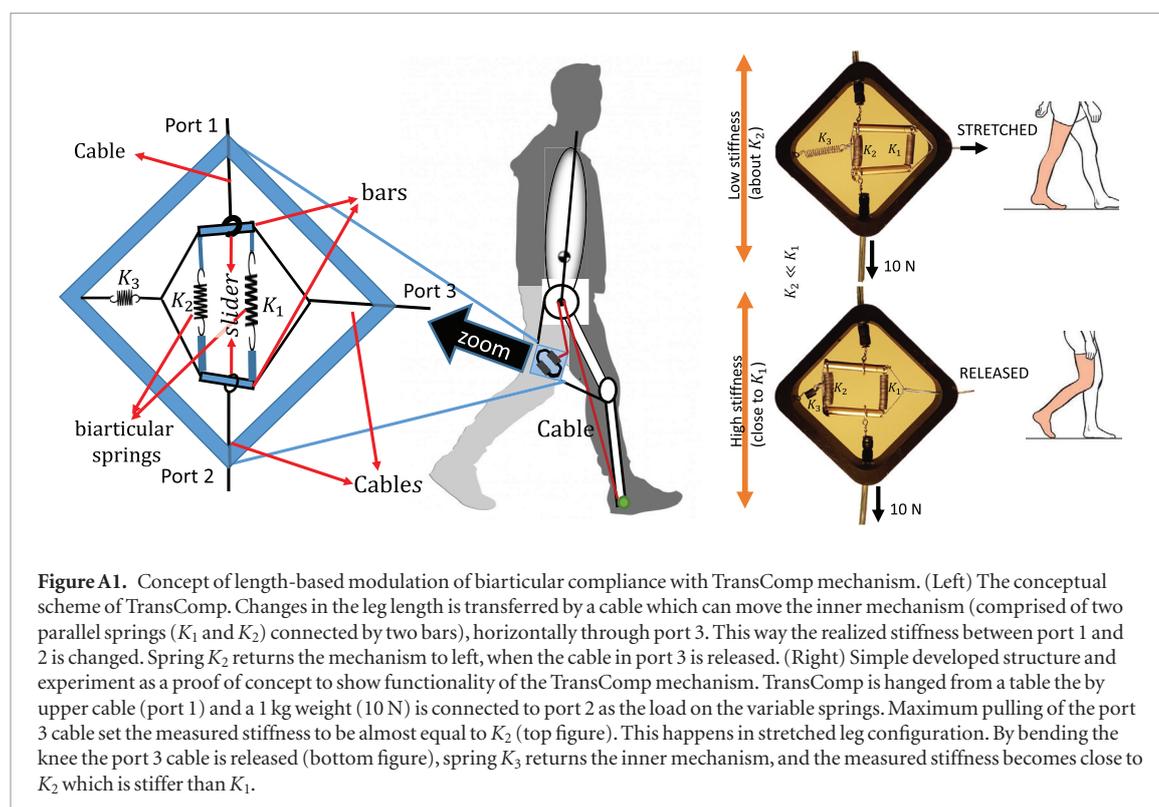
Figure A1. Concept of length-based modulation of biarticular compliance with TransComp mechanism. (Left) The conceptual scheme of TransComp. Changes in the leg length is transferred by a cable which can move the inner mechanism (comprised of two parallel springs (K_1 and K_2) connected by two bars), horizontally through port 3. This way the realized stiffness between port 1 and 2 is changed. Spring K_2 returns the mechanism to left, when the cable in port 3 is released. (Right) Simple developed structure and experiment as a proof of concept to show functionality of the TransComp mechanism. TransComp is hanged from a table the by upper cable (port 1) and a 1 kg weight (10 N) is connected to port 2 as the load on the variable springs. Maximum pulling of the port 3 cable set the measured stiffness to be almost equal to K_2 (top figure). This happens in stretched leg configuration. By bending the knee the port 3 cable is released (bottom figure), spring K_3 returns the inner mechanism, and the measured stiffness becomes close to K_2 which is stiffer than K_1.

required energy to keep the stiffness or to switch from one stiffness to another will be minimized. For this, we need to set high and low values, respectively, for static and kinetic friction between the slider and the bar. It is noteworthy that the proposed mechanism can also support loading and unloading of the stance leg. When the stance leg is loaded (first half of stance phase) and the (virtual) leg is shortened, the potential energy provided by gravity can be stored in the TransComp, by increasing the stiffness. During unloading of the leg (second half of the stance phase) which results in leg lengthening, the stiffness reduction in TransComp can support body upward movement. However, fine tuning of this system to deliver the prescribed formulation (equation (6)) is critical. This is a proof of concept to show the functionality of the mechanism. Indeed, to deliver an applicable tool to be used in the exosuit, further attempts are required.

ORCID iDs

Hamid Barazesh ⬦ https://orcid.org/0000-0002-1061-6920
Maziar Ahmad Sharbafi ⬦ https://orcid.org/0000-0001-5727-7527

References

[1] Tudor-Locke C, Johnson W D and Katzmarzyk P T 2009 Accelerometer-determined steps per day in US adults *Med. Sci. Sports Exerc.* **41** 1384–91

[2] Herr H 2009 Exoskeletons and orthoses: classification, design challenges and future directions *J. Neuroeng. Rehabil.* **6** 21

[3] Zahedi M S, Sykes A J, Lang S T, Chas A Blatchford and Sons Ltd 2003 Lower limb prosthesis *US Patent* 6517585

[4] Hong Y W, King Y, Yeo W, Ting C, Chuah Y, Lee J and Chok E T 2013 Lower extremity exoskeleton: review and challenges surrounding the technology and its role in rehabilitation of lower limbs *Aust. J. Basic Appl. Sci.* **7** 520–4

[5] Chen B, Ma H, Qin L, Gao F, Chan K, Law S, Qin L and Liao W 2016 Recent developments and challenges of lower extremity exoskeletons *J. Orthopaedic Trans.* **5** 26–37

[6] Alcobendas-Maestro M, Esclarín-Ruz A, Casado-López R M, Muñoz-González A, Perez-Mateos G, Gonzalez-Valdizan E and Martin J L R 2012 Lokomat robotic-assisted versus overground training within 3 to 6 m of incomplete spinal cord lesion: randomized controlled trial *Neurorehabilitation Neural Repair* **26** 1058–63

[7] Banala S K, Agrawal S K and Scholz J P 2007 Active leg exoskeleton (alex) for gait rehabilitation of motor-impaired patients *IEEE 10th Int. Conf. on Rehabilitation Robotics* (IEEE) pp 401–7

[8] Riener R, Lunenburger L, Jezernik S, Anderschitz M, Colombo G and Dietz V 2005 Patient-cooperative strategies for robot-aided treadmill training: first experimental results *IEEE Trans. Neural Syst. Rehabil. Eng.* **13** 380–94

[9] Esquenazi A, Talaty M, Packel A and Saulino M 2012 The rewalk powered exoskeleton to restore ambulatory function to individuals with thoracic-level motor-complete spinal cord injury *Am. J. Phys. Med. Rehabil.* **91** 911–21

[10] Tsukahara A, Kawanishi R, Hasegawa Y and Sankai Y 2010 Sit-to-stand and stand-to-sit transfer support for complete paraplegic patients with robot suit HAL *Adv. Robot.* **24** 1615–38

[11] Ikeuchi Y, Ashihara J, Hiki Y, Kudoh H and Noda T 2009 Walking assist device with bodyweight support system *IEEE/RSJ Int. Conf. on Intelligent Robots and Systems* (IEEE) pp 4073–9

[12] Zoss A B, Kazerooni H and Chu A 2006 Biomechanical design of the Berkeley lower extremity exoskeleton (BLEEX) *IEEE/ASME Trans. Mechatronics* **11** 128–38

[13] Zhang J, Fiers P, Witte K A, Jackson R W, Poggensee K L, Atkeson C G and Collins S H 2017 Human-in-the-loop optimization of exoskeleton assistance during walking *Science* **356** 1280–4

[14] Quinlivan B *et al* 2017 Assistance magnitude versus metabolic cost reductions for a tethered multiarticular soft exosuit *Sci. Robot.* **2** 4416

[15] Mooney L M and Herr H M 2016 Biomechanical walking mechanisms underlying the metabolic reduction caused by an autonomous exoskeleton *J. Neuroeng. Rehabil.* **13** 4

[16] Seo K, Lee J, Lee Y, Ha T and Shim Y 2016 Fully autonomous hip exoskeleton saves metabolic cost of walking *IEEE Int. Conf. on Robotics and Automation* (IEEE) pp 4628–35

[17] Ding Y, Kim M, Kuindersma S and Walsh C J 2018 Human-in-the-loop optimization of hip assistance with a soft exosuit during walking *Sci. Robot.* **3** eaar5438

[18] Kim J *et al* 2019 Reducing the metabolic rate of walking and running with a versatile, portable exosuit *Science* **365** 668–72

[19] Nasiri R, Ahmadi A and Ahmadabadi M N 2018 Reducing the energy cost of human running using an unpowered exoskeleton *IEEE Trans. Neural Syst. Rehabil. Eng.* **26** 2026–32

[20] Xiong C, Zhou T, Zhou L, Wei T and Chen W 2019 Multi-articular passive exoskeleton for reducing the metabolic cost during human walking *2019 Wearable Robotics Association Conf. (WearRAcon)* (IEEE) pp 63–7

[21] Collins S H, Wiggin M B and Sawicki G S 2015 Reducing the energy cost of human walking using an unpowered exoskeleton *Nature* **522** 212

[22] Asbeck A T, De Rossi S M, Holt K G and Walsh C J 2015 A biologically inspired soft exosuit for walking assistance *Int. J. Robot. Res.* **34** 744–62

[23] Nasiri R, Rayati M and Ahmadabadi M N 2019 Feedback from mono-articular muscles is sufficient for exoskeleton torque adaptation *IEEE Trans. Neural Syst. Rehabil. Eng.* **27** 2097–106

[24] Firouzi V, davoodi A, Bahrami F and Sharbafi M N D From a biological template model to gait assistance with an exosuit *Frontiers Neurorobotics* (under review)

[25] Sharbafi M A, Seyfarth A and Zhao G 2017 Locomotor sub-functions for control of assistive wearable robots *Frontiers Neurorobotics* **11** 44

[26] Sharbafi M A, Barazesh H, Iranikhah M and Seyfarth A 2018 Leg force control through biarticular muscles for human walking assistance *Frontiers Neurorobotics* **12** 39

[27] Maus H M, Lipfert S, Gross M, Rummel J and Seyfarth A 2010 Upright human gait did not provide a major mechanical challenge for our ancestors *Nat. Commun.* **1** 1–6

[28] Geyer H and Her H 2010 A muscle-reflex model that encodes principles of legged mechanics produces human walking dynamics and muscle activities *IEEE Trans. Neural Syst. Rehabil. Eng.* **18** 263–73

[29] Walsh C J, Endo K and Herr H 2007 A quasi-passive leg exoskeleton for load-carrying augmentation *Int. J. Humanoid Robot.* **4** 487–506

[30] Blickhan R 1989 The spring-mass model for running and hopping *J. Biomech.* **22** 1217–27

[31] Geyer H, Seyfarth A and Blickhan R 2006 Compliant leg behaviour explains basic dynamics of walking and running *Proc. R. Soc.* B **273** 2861–7

[32] Sharbafi M A, Lee D, Kiemel T and Seyfarth A 2017 Fundamental subfunctions of locomotion *Bioinspired Legged Locomotion* (Oxford: Butterworth-Heinemann) pp 11–53

[33] Full R J and Koditschek D E 1999 Templates and anchors: neuromechanical hypotheses of legged locomotion on land *J. Exp. Biol.* **202** 3325–32

[34] Seipel J, Kvalheim M, Revzen S, Sharbafi M A and Seyfarth A 2017 Conceptual models of legged locomotion *Bioinspired Legged Locomotion* (Oxford: Butterworth-Heinemann) pp 55–131

[35] Lipfert S W 2010 *Kinematic and Dynamic Similarities Between Walking and Running* (Hamburg: Verlag Dr Kovaĉ)

[36] Seyfarth A, Geyer H, Guenther M and Blickhan R 2002 A movement criterion for running *J. Biomech.* **35** 649–55

[37] Maus H M, Rummel J and Seyfarth A 2008 Stable upright walking and running using a simple pendulum based control scheme *Int. Conf. of Climbing and Walking Robotics* pp 623–9

[38] Seyfarth A, Geyer H and Herr H 2003 Swing-leg retraction: a simple control model for stable running *J. Exp. Biol.* **206** 2547–55

[39] Sharbafi M A, Maufroy C, Ahmadabadi M N, Yazdanpanah M J and Seyfarth A 2013 Robust hopping based on virtual pendulum posture control *Bioinspiration Biomimetics* **8** 036002

[40] Sharbafi M A and Seyfarth A 2014 Stable running by leg force-modulated hip stiffness *IEEE Int. Conf. on Biomedical Robotics and Biomechatronics* pp 204–10

[41] Sharbafi M A and Seyfarth A 2015 Fmch: a new model for human-like postural control in walking *IEEE/RSJ Int. Conf. on Intelligent Robots and Systems* (IEEE) pp 5742–7

[42] Hill A V 1938 The heat of shortening and the dynamic constants of muscle *Proc. R. Soc.* B **126** 136–95

[43] Davoodi A, Mohseni O, Seyfarth A and Sharbafi M A 2019 From template to anchors: transfer of virtual pendulum posture control balance template to adaptive neuromuscular gait model increases walking stability *R. Soc. Open Sci.* **6** 181911

[44] Sharbafi M A, Rode C, Kurowski S, Scholz D, Möckel R, Radkhah K, Zhao G, Rashty A M, von Stryk O and Seyfarth A 2016 A new biarticular actuator design facilitates control of leg function in biobiped3 *Bioinspiration Biomimetics* **11** 046003

[45] Braun D J, Chalvet V, Chong T H, Apte S S and Hogan N 2019 Variable stiffness spring actuators for low-energy-cost human augmentation *IEEE Trans. Robot.* **35** 1435–49

[46] Hogan N 1985 Impedance control: an approach to manipulation *J. Dyn. Sys. Meas. Control* **107** 1–7

[47] Geyer H, Seyfarth A and Blickhan R 2003 Positive force feedback in bouncing gaits? *Proc. R. Soc.* B **270** 2173–83

[48] Song S and Geyer H 2015 A neural circuitry that emphasizes spinal feedback generates diverse behaviours of human locomotion *J. Physiol.* **593** 3493–511

[49] Krishnaswamy P, Brown E N and Herr H M 2011 Human leg model predicts ankle muscle-tendon morphology, state, roles and energetics in walking *PLoS Comput. Biol.* **7** e1001107

[50] Alexander R McN 1997 Optimum muscle design for oscillatory movements *J. Theor. Biol.* **184** 253–9

[51] Asbeck A T, De Rossi S M, Galiana I, Ding Y and Walsh C J 2014 Stronger, smarter, softer: next-generation wearable robots *IEEE Robot. Autom. Mag.* **21** 22–33

[52] Schmidt K, Duarte J E, Grimmer M, Sancho-Puchades A, Wei H, Easthope C S and Riener R 2017 The myosuit: Bi-articular anti-gravity exosuit that reduces hip extensor activity in sitting transfers *Frontiers Neurorobotics* **11** 57

[53] Seyfarth A, GuÈnther M and Blickhan R 2001 Stable operation of an elastic three-segment leg *Biol. Cybern.* **84** 365–82

[54] van Ingen Schenau G J, Bobbert M F and van Soest A J 1990 The unique action of bi-articular muscles in leg extensions *Multiple Muscle Systems* (Berlin: Springer) pp 639–52

[55] Dembia C L, Silder A, Uchida T K, Hicks J L and Delp S 2017 Simulating ideal assistive devices to reduce the metabolic cost of walking with heavy loads *PLoS One* **12** e0180320

[56] Cleland J 1867 On the actions of muscles passing over more than one joint *J. Anat. Physiol.* **1** 85

[57] Fenn W 1938 The mechanics of muscular contraction in man *J. Appl. Phys.* **9** 165–77

[58] Sarmadi A, Schumacher C, Seyfarth A and Sharbafi M A 2019 Concerted control of stance and balance locomotor subfunctions-leg force as a conductor *IEEE Trans. Med. Robot. Bionics* **1** 49–57

[59] Jacobs R and van Ingen Schenau G 1992 Control of an external force in leg extensions in humans *J. Physiol.* **457** 611–26

[60] Cleather D J, Southgate D F and Bull A M 2015 The role of the biarticular hamstrings and gastrocnemius muscles in closed chain lower limb extension *J. Theor. Biol.* **365** 217–25

[61] Winter D A 2005 *BioMechanics and Motor Control of Human Movement* 3 edn (New York: John Wiley & Sons)

[62] Torres-Oviedo G and Ting L H 2010 Subject-specific muscle synergies in human balance control are consistent across different biomechanical contexts *Am. J. Physiol. Heart. Circ. Physiol.* **103** 3084–98

[63] Beck O N, Punith L K, Nuckols R W and Sawicki G S 2019 Exoskeletons improve locomotion economy by reducing active muscle volume *Exercise Sport Sci. Rev.* **47** 237–45

[64] Schumacher C, Berry A, Lemus D, Rode C, Seyfarth A and Vallery H 2019 Biarticular muscles are most responsive to upper-body pitch perturbations in human standing *Sci. Rep.* **9** 1–14

[65] Nilsson, Thorstensson A J and Halbertsma J 1985 Changes in leg movements and muscle activity with speed of locomotion and mode of progression in humans *Acta Physiol. Scand.* **123** 457–75

[66] Poggensee K L, Sharbafi M A and Seyfarth A 2014 Characterizing swing-leg retraction in human locomotion *Mobile Service Robotics* (Singapore: World Scientific) pp 377–84

[67] Simonsen E B, Thomsen L and Klausen K 1985 Activity of mono-and biarticular leg muscles during sprint running *European J. Appl. Physiol. Occup. Physiol.* **54** 524–32

[68] Burdet E, Osu R, Franklin D W, Milner T E and Kawato M 2001 The central nervous system stabilizes unstable dynamics by learning optimal impedance *Nature* **414** 446

[69] Günther M and Blickhan R 2002 Joint stiffness of the ankle and the knee in running *J. Biomech.* **35** 1459–74

[70] Sharbafi M A, Rashty A M N, Rode C and Seyfarth A 2017 Reconstruction of human swing leg motion with passive biarticular muscle models *Hum. Mov. Sci.* **52** 96–107

[71] Bai S, Virk G S and Sugar T 2018 *Wearable Exoskeleton Systems: Design, Control and Applications* (Stevenage: Institution of Engineering and Technology)

[72] Geyer H, Thatte N and Duan H 2017 Toward balance recovery with active leg prostheses using neuromuscular model control *Converging Clinical and Engineering Research on Neurorehabilitation II'* (Berlin: Springer) pp 649–52

[73] Walsh C 2018 Human-in-the-loop development of soft wearable robots *Nat. Rev. Mater.* **3** 78

[74] Van Ham R, Vanderborght B, Van Damme M, Verrelst B and Lefeber D 2007 MACCEPA, the mechanically adjustable compliance and controllable equilibrium position actuator: design and implementation in a biped robot *Robot. Auton. Syst.* **55** 761–8

[75] Vanderborght B *et al* 2013 Variable impedance actuators: a review *Robot. Auton. Syst.* **61** 1601–14

[76] Shahri M A, Mohseni O, Bidgoly H J and Ahmadabadi M N 2020 Profile design of parallel rotary compliance for energy efficiency in cyclic tasks *IEEE/ASME Trans. Mechatronics* **25** 142–51